Structure and Electrical Properties of the Oriented Polyaniline Films

MEIXIANG WAN,[1,*] MING LI,[1] JUNCHAO LI,[1] and ZHENXING LIU[2]

[1]Institute of Chemistry, Academia Sinica, Beijing 100080, People's Republic of China; [2]Institute of Physics, Chinese Academy of Sciences, Beijing 100080, People's Republic of China

SYNOPSIS

The structure of oriented polyaniline (PANI) films were characterized by elemental analysis, FTIR, XPS, SEM, and X-ray diffraction, and their electrical properties were measured as a function of the protonation state, elongation ratio, temperature, and applied pressure. A maximum conductivity at room temperature for oriented PANI films can be achieved up to 500 s/cm with conductivity anisotropy as high as 20 : 1. The temperature dependence of conductivity for both unoriented and oriented films at 77–300 K and applied pressure of 0–11.4 kbar is consistent with the 3-D variable-range hopping model; however, the hopping barrier of oriented films is one order magnitude lower than that of unoriented films. The mechanism of enhanced conductivity for oriented PANI films is discussed. © 1994 John Wiley & Sons, Inc.

INTRODUCTION

Since the emeraldine base form of polyaniline (PANI) is readily solution processible and it may be cast as free-standing film, it is possible to obtain oriented PANI films. Cromack et al.[1] first reported that oriented PANI films can be obtained by heating them above the glass transition temperature (> 110°C) and this work was reported in detail.[2,3] Moreover, Monkman and Adams[4] reported that the conductivity of the oriented PANI film was able to achieve up to 350 s/cm with conductivity anisotropy as high as 24 : 1. They suggested that the increased conductivity for oriented PANI film was due to the increase of chain length and higher conjugation. On the other hand, Scherr et al.[3] believed that the increased conductivity for oriented PANI film may be due to the increase of the degree of crystallinity. As described above, the mechanism of enhanced conductivity for oriented PANI film is not understood yet.

In this article, the structure of oriented PANI films was examined by elemental analysis, FTIR, XPS, SEM, and X-ray diffraction and their electrical properties were measured as a function of the protonation state, elongation ratio, temperature, and pressure in order to understand the mechanism of enhanced conductivity for oriented PANI films.

EXPERIMENTAL

The emeraldine base powder was synthesized by a chemical method reported by MacDiarmid et al.[5] The film of the emeraldine base form of PANI was prepared by evaporating the solution of the emeraldine base in NMP at 70–80°C as described in a previous article.[6] Oriented PANI film was obtained by a home-made drawing meter at about 80°C. The elongation ratio was determined by l/l_0, where l and l_0 are the length of samples for oriented and unoriented films, respectively. Oriented PANI films with different protonation states were obtained by treating their base form with aqueous HCl solutions of different acidity. The degree of the protonation state was determined by the pH value, which was measured by a pH meter (S-10A Model). Normal and polarized FTIR were recorded on a ES-300 electron spectrometer. X-ray diffraction was determined by a Rigaku model at an applied voltage of $V = 40$

* To whom correspondence should be addressed.

Journal of Applied Polymer Science, Vol. 53, 131–139 (1994)
 CCC 0021-8995/94/020131-09

kV, I = 30 mA, and scanning speed of 2 degrees/min using a copper target. The SEM morphology was examined with a Hitachi s-530 scanning electron microscope. The electrical properties of PANI films were measured as a function of the elongation ratio, the protonation state, temperature, and applied pressure. The temperature dependence of conductivity at 77–300 K and applied pressure of 0–11.4 kbar was measured by a four-probe method.

RESULTS AND DISCUSSION

Structure Characterization

Results of the elemental analysis indicate that the atomic ratio of carbon to nitrogen for oriented PANI films is in agreement with the results calculated from molecular formula of PANI and their composition is similar to unoriented samples. This suggests that the drawing processes under heating for PANI film does not change their composition, which is consistent with XPS measurement in that there is no difference in the chemical shift of N_{1s}, O_{1s}, and Cl_{2p} between oriented and unoriented films. No significant difference in positions of characteristic peaks of oriented PANI films compared with unoriented films in FTIR spectra was observed, as shown in Figure 1(a). The assignment of IR absorption is consistent with observations obtained by Monkman and Adams.[4] These results indicate that the main-chain structure of the oriented films is unchanged after the drawing treatment. However, experiment results of polarized FTIR spectra of oriented PANI films show that the chains are oriented along the stretching direction. Typical polarized FTIR spectra of oriented PANI films are shown in Figure 1(b) and (c). The absorption intensity of the main characteristic IR bands with a different polarized direction for oriented PANI films (l/l_0 = 3) is summarized in Table I. One can see that the polarized FTIR spectra of oriented PANI films show a significant infrared dichroism. The dichroic ratio is defined as $R = A_{\parallel}/A_{\perp}$, where $A_{\parallel}$ and $A_{\perp}$ are the absorption intensity of which the stretched film is placed parallel or perpendicular to the polarized light, respectively. The results show that the dichroic ratio of the vibrations along the chain is over 1, whereas that of vibrations perpendicular to the chain is less than 1. These results demonstrated that the chains were oriented along the elongation direction after the drawing process. This is consistent with observations obtained by Cromack et al.[2]

Typical scanning electronic micrographs of the surface and the cross section of oriented films compared with unoriented films are shown in Figure 2. For unoriented PANI films, their surface SEM images show a granular morphology [see Fig. 2(a1)], whereas its cross-section SEM images appear as a meshlike morphology composed with granulars [see Fig. 2(a2)]. For oriented PANI films (l/l_0 = 3), the granulars on the surface SEM images are oriented

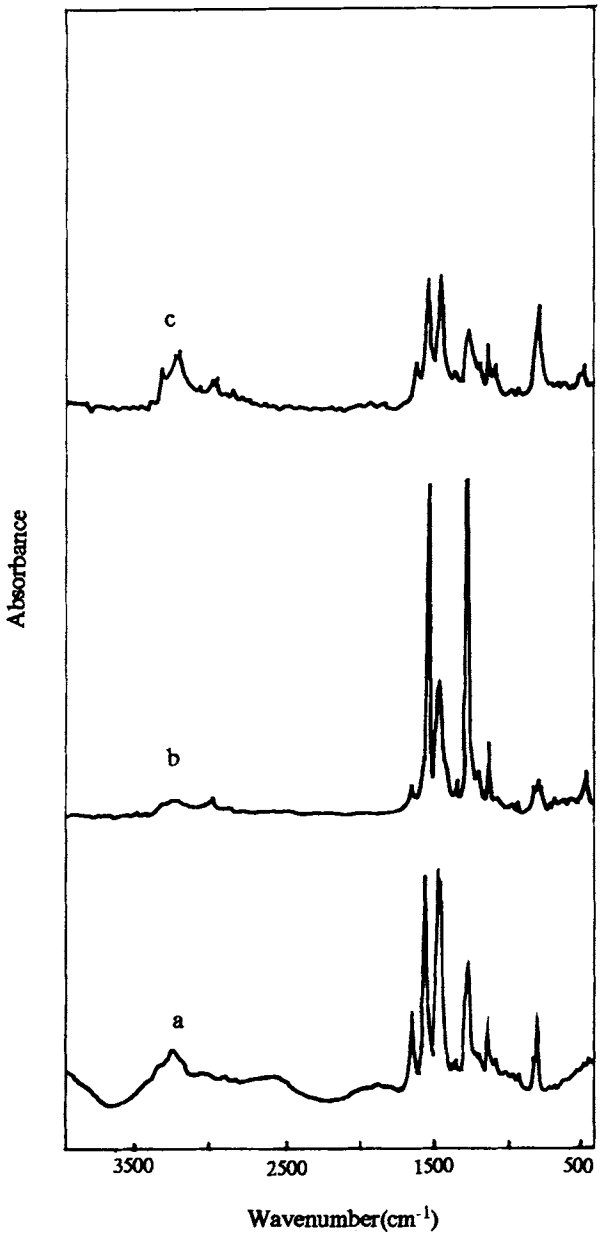

Figure 1 Normal and polarized FTIR spectra of oriented PANI films, d = 7 μm, l/l_0 = 3, emeraldine base form: (a) normal FTIR spectra; (b) polarized FTIR spectra, parallel to stretching direction (180°); (c) polarized FTIR spectra, perpendicular to stretching direction (90°).

Table I. The Absorbance Intensity of the Main Characteristic IR Bands with Different Polarized Directions for Oriented PANI Films

IR Bands (cm^{-1})	Absorbance 180°	Absorbance 90°	R ($\parallel/\perp$)
3385(N—H)	0.19	0.35	0.54
3287(=NH)	0.24	0.48	0.5
3028(C—H)	0.28	0.24	1.2
1593(N=Q=N)	5.7	1.6	3.6
1505(N—B—N)	2.3	1.6	1.4
1311(QBB QBQ)	5.6	0.9	6.2
1170(C—N)	1.2	0.53	2.2
834(C—H)	0.66	1.6	0.41

along the elongation direction [see Fig. 2(b1)]; at the same time, the meshlike morphology on cross section SEM images disappears and the granulars begin to orient along the elongation direction [see Fig. 2(b2)].

A comparison of the X-ray diffraction of oriented PANI films ($l/l_0 = 3$) with unoriented films is shown in Figure 3. For unoriented PANI films, a broad weak reflection near $2\theta = 19°$ was observed, which shows that the unoriented PANI films exhibit an amorphous structure. For oriented PANI films, however, two strong reflection peaks at $2\theta = 19.22°$ and 23.08° were observed, which is consistent with observations reported by Scherr et al.[3] and Pouget et al.[7] Moon et al.[8] suggested that the relatively narrow reflection

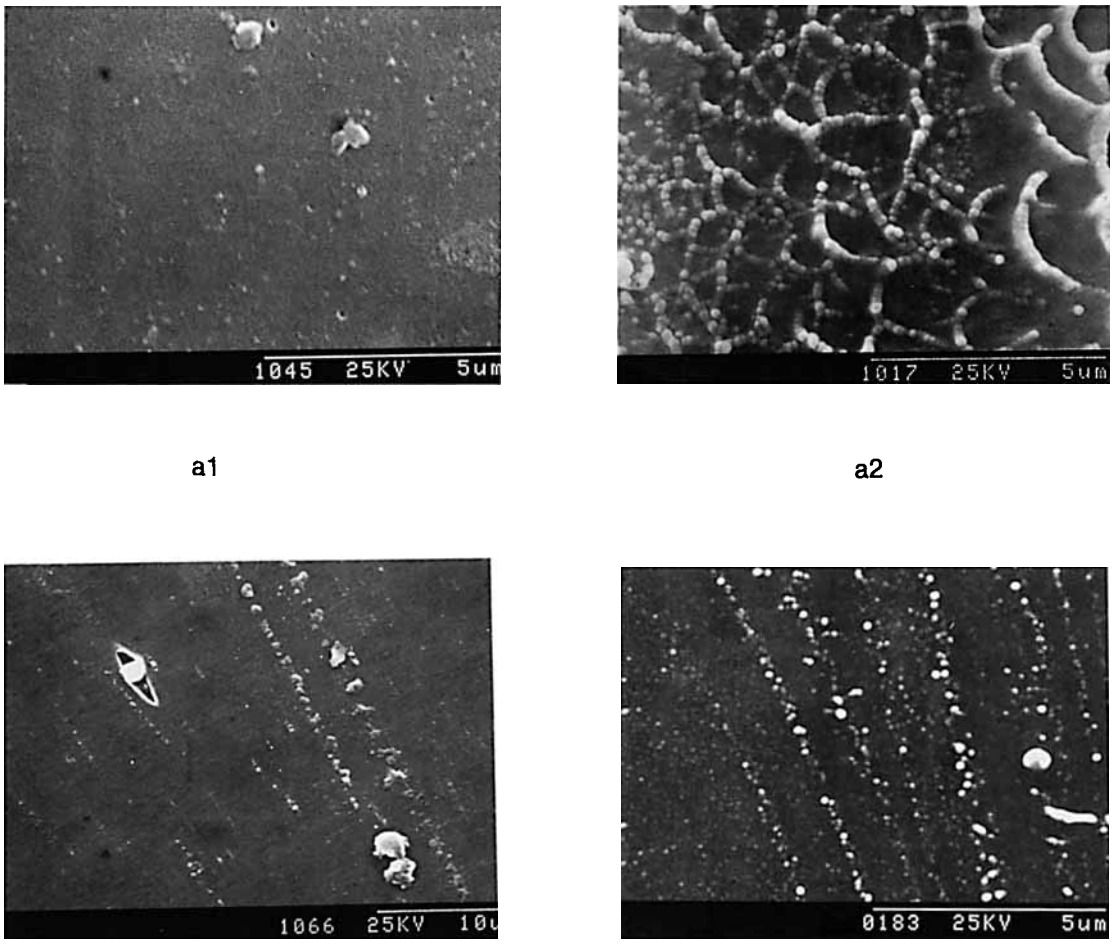

Figure 2 Scanning electronic micrographs of the emeraldine base form of PANI films. (a) Unoriented film: (1) surface, (2) cross section; (b) oriented film, $l/l_0 = 3$: (1) surface, (2) cross section.

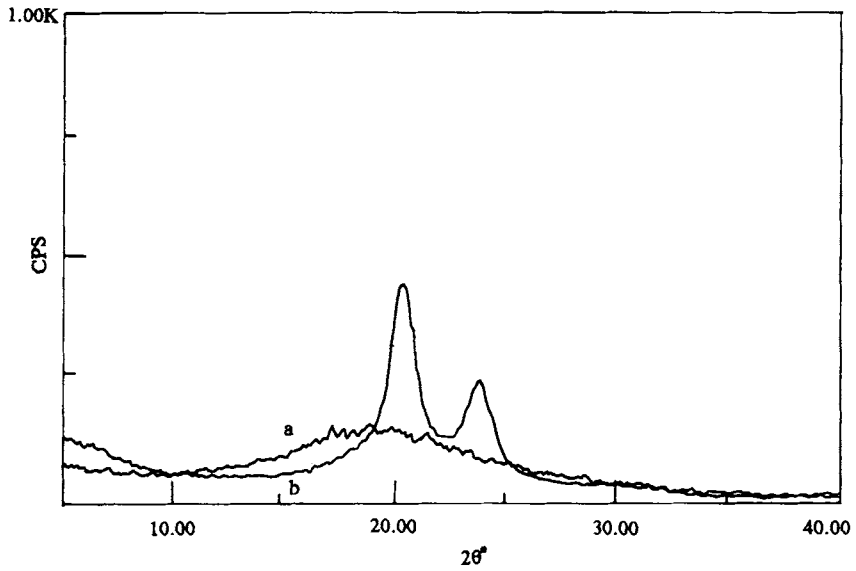

Figure 3 X-ray diffraction of PANI films: (a) unoriented film; (b) oriented film ($l/l_0 = 3$).

at $2\theta = 10°$ was caused by scattering with momentum transfer approximately parallel to the PANI chain, whereas the two strongest peaks at $2\theta = 19.5°$ and 22.8° were due to the scattering of interchain packing. In our X-ray diffraction as shown in Figure 3, the low-angle reflection (2θ near 10°) was not seen, whereas the two reflection peaks (2θ near 19.22° and 23.08°) for oriented PANI film were obviously observed, which indicates that the orientation of interchain packing is expected after the drawing process. Based on the results obtained from the polarized FTIR, SEM, and X-ray diffraction of oriented PANI films, it might be concluded that a period arrangement of the chain and/or interchain along the elongation direction exists.

Electrical Properties

A typical dependence of the conductivity of oriented PANI films on the elongation ratio at room temperature is shown in Figure 4. It is clearly seen that the conductivity parallel to the elongation direction is nearly in a linear relationship to the elongation ratio. On the other hand, the conductivity perpendicular to the elongation direction is independent of the elongation ratio. A maximum conductivity at

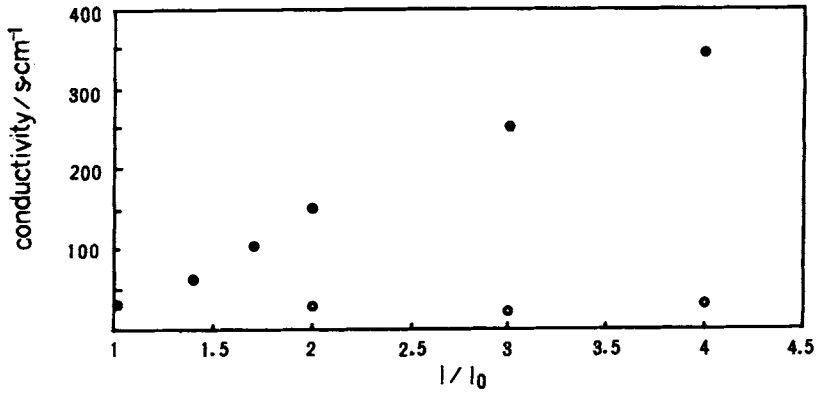

Figure 4 The conductivity of oriented PANI films at room temperature as a function of the elongation ratio: (●) parallel to stretching direction, pH 0; (○) perpendicular to stretching direction, pH 0.

room temperature for oriented PANI films is able to achieve up to 500 s/cm with conductivity anisotropy as high as 20 : 1, which is consistent with the highest conductivity value of 400 s/cm for 1 : 4 stretched samples reported by Wang et al.[9]

The relationship between the conductivity at room temperature and the protonation state for oriented and unoriented PANI films is shown in Figure 5. It is shown that an insulator-to-metal transition upon the protonation state for oriented PANI films was observed, which is consistent with observations from unoriented films.[10,11] However, it is noted that the conductivity of oriented PANI films is as same as that of unoriented films when the pH value is higher than 2, whereas a significant difference in conductivity between oriented and unoriented films was observed at a lower pH value.

Temperature dependence of the conductivity of both oriented and unoriented PANI films protonated by HCl (pH 0) at an applied pressure of 0–11.4 kbar was measured. In general, the variable range hopping

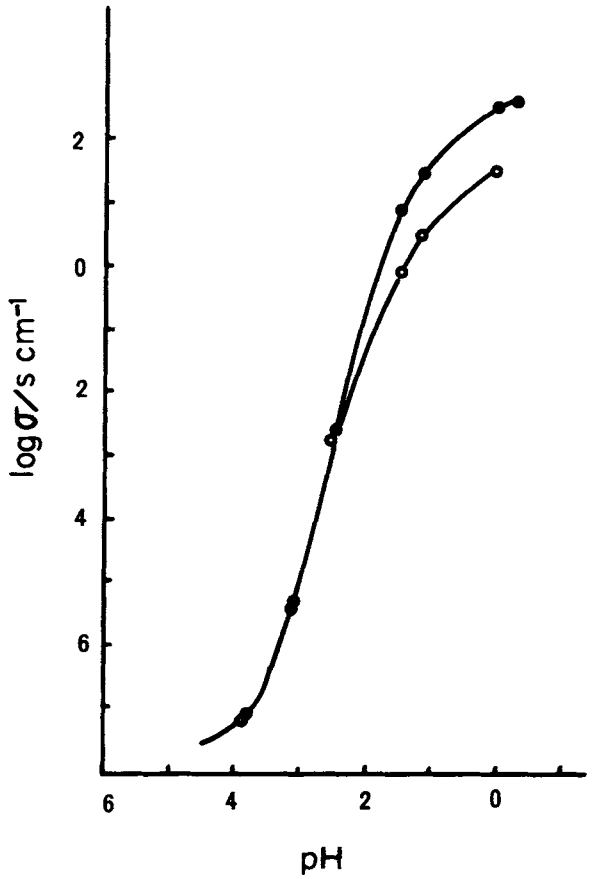

Figure 5 Conductivity of PANI films at room temperature as a function of the protonation states: (○) unoriented films; (●) oriented films, $l/l_0 = 3$.

model proposed by Mott and Davis[12] is used to explain the temperature dependence of conductivity of disordered materials; it can be expressed as

$$\sigma(T) = \sigma_0 T^{-1/2} \exp[-(T_0/T)^{1/4}] \qquad (1)$$

where σ_0 is a constant; T_0, the hopping barrier, and T, Kelvin temperature. Our experimental data are best fit to the relationship of $\ln[\sigma T^{1/2}]$ plotted to $T^{-1/4}$ as shown in Figure 6; the σ_0 and T_0 values calculated at different applied pressures are given in Table II. Based on these results, it is, thus, reasonable to believe that the temperature dependence of the conductivity for both oriented and unoriented PANI films is consistent with the 3-D VRH model.[12] Compared with Wang et al.'s[13-14] results, a difference in the model used and different T_0 values are observed; this may be due to a difference in stretching conditions. In Wang et al.'s experiment, e.g., the PANI films were stretched at above the glass transition temperature (110–140°C); in contrast, the temperature that we used was about 80°C.

In addition, it is noted that the T_0 value of oriented PANI films at a given applied pressure is one order magnitude lower than that of unoriented films. This suggests that the hopping barrier for oriented films decreases after the drawing treatment, which is consistent with observations that the chain and/or interchain packing is oriented along the elongation direction after stretching. Moreover, the conductivity of unoriented PANI films increases with increase of the applied pressure, whereas a maximum conductivity for oriented PANI films near 4.7 kbar was observed, as shown in Figure 7. The reason why the conductivity of oriented PANI films decreases with increase of the applied pressure when the applied pressure is higher than 4.7 kbar is not understood yet.

Mechanism of the Enhanced Conductivity

Many mechanisms of temperature dependence of conducting polymers have been proposed, such as VRH,[12] metallic islands,[15] doping defects,[16] and change energy limited tunneling (CELT).[17,18] Moreover, the mechanism of conductivity anisotropy in conducting polymers has been reported.[19-20] In this article, we proposed a simple model of the series of the chain resistance and interchain resistance to explain the enhanced conductivity of stretched PANI films.

As is known, the conductivity, σ, is expressed as

$$\sigma = ne\mu \qquad (2)$$

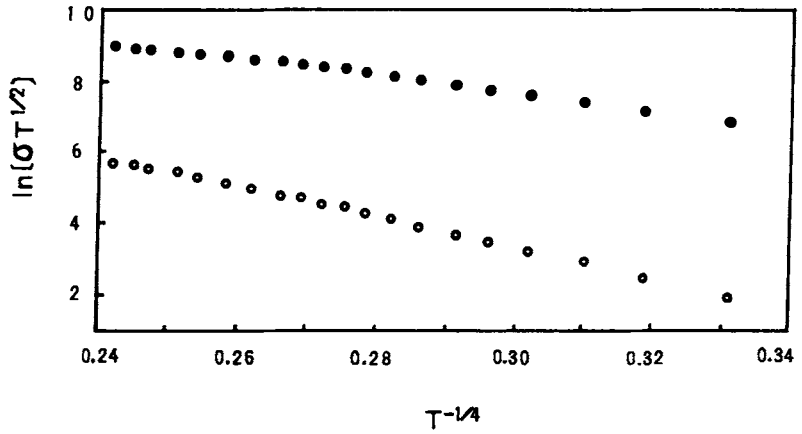

Figure 6 Temperature dependence of the conductivity of PANI films: (○) unoriented film, pH 0; (●) oriented film, $l/l_0 = 3$, pH 0.

where n is the density of charge carriers; e, the electron charge; and μ, the mobility of charge carriers. For conducting polymers, the density of charge carriers for given conducting polymers is mainly dependent on the doping level. Thus, it is expected that the enhanced conductivity for stretched conducting polymers at a given doping level might be totally controlled by the increase of the mobility of the charge carriers. Moreover, the scanning electronic microscopy (SEM) of conducting polymers shows fibrillar or granular morphology, and it has been demonstrated that the fibrillar or granular itself is metal, which is surrounded by insulator materials called "the conducting island." [15] Ginder et al.[21] reported that the conductivity of the "conducting island" of PANI itself could be achieved up to 10^3 s/cm. This suggested that microscopic localized state or interfibrillar and intergranular barriers are present. Furthermore, the temperature dependence of conductivity measured by a standard four-probe method for conducting polymers never shows a metallic temperature dependence of conductivity, whereas it always exhibits a semiconducting behavior, which obeys a variable-range hopping model.[12] This is attributed to the contact resistance between interfibrillar or intergranular regions of conducting polymers. It has been demonstrated that a metallic temperature dependence of conductivity of doped conducting polymers could be observed if the interfibrillar or intergranular resistance is eliminated by the shorted voltage compaction (VSC) method.[22,23] For example, the metallic temperature dependence of conducting polymers, such as polyacetylene,[24] polypyrrole,[25] polythiophene,[26] and polyaniline,[6] has been observed by the VSC conductivity method. Based on the discussion above, therefore, the interchain conductivity should be considered for the conductivity of conducting polymers, and both the conductivity on the chain and the interchain conductivity between chains contribute to the conductivity of the conducting polymers. We proposed that the measured resistance (R_m) of conducting polymers is a series of chain resistance (R_c) and interchain resistance (R_i); then, it can be expressed as

$$R_m = R_c + R_i \tag{3}$$

Table II. T_0 Value at Different Applied Pressures for Unoriented and Oriented PANI Films

	Applied Pressure (kbar)			
	0	3.5	7.1	11.4
	T_0 (K)			
Unoriented	3.11×10^6	2.52×10^6	2.35×10^6	1.17×10^6
Oriented	3.31×10^5	2.40×10^5	2.25×10^5	3.03×10^5

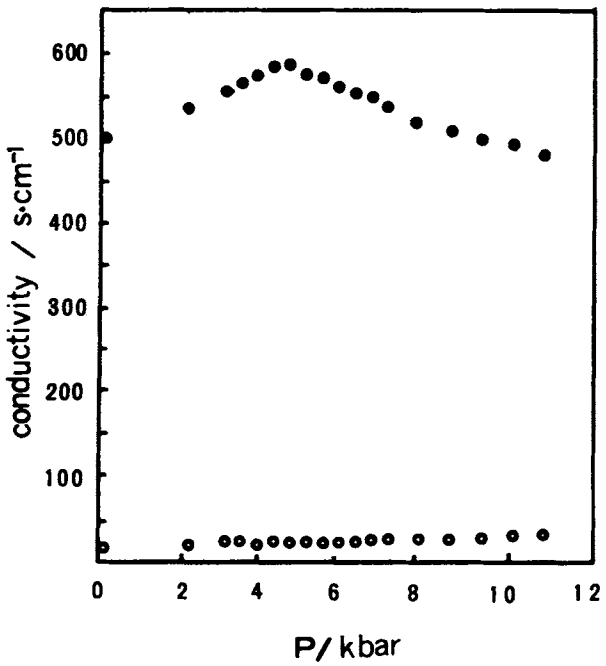

Figure 7 Pressure dependence of the conductivity of PANI films at room temperature: (○) unoriented film, pH 0; (●) oriented film, $l/l_0 = 4$, pH 0.

and

$$R = \rho \cdot \frac{L}{S} \tag{3a}$$

$$\rho = \frac{1}{\sigma} \tag{3b}$$

where ρ and σ is resistivity and conductivity, respectively. L is the distance between electrodes, and S, the surface area of the cross section of the sample. If eqs. (3a) and (3b) substitute for eq. (3), then

$$\left(\frac{1}{\sigma}\cdot\frac{L}{S}\right)_m = \frac{1}{\sigma_c}\cdot\left(\frac{L}{S}\right)_c + \frac{1}{\sigma_i}\cdot\left(\frac{L}{S}\right)_i \tag{4}$$

or

$$\left(\frac{1}{\sigma}\right)_m = \frac{1}{\sigma_c}\cdot\left(\frac{S}{L}\right)_m\cdot\left(\frac{L}{S}\right)_c + \frac{1}{\sigma_i}\cdot\left(\frac{S}{L}\right)_m\cdot\left(\frac{L}{S}\right)_i \tag{5}$$

let

$$\left(\frac{S}{L}\right)_m\cdot\left(\frac{L}{S}\right)_c = a \tag{5a}$$

$$\left(\frac{S}{L}\right)_m\cdot\left(\frac{L}{S}\right)_i = b \tag{5b}$$

thus,

$$\sigma_m = \frac{\sigma_c\sigma_i}{a\sigma_i + b\sigma_c} \tag{6}$$

Equation (6) is a mathematical expression of the physical model proposed in this article. $(S/L)_m$ can be measured by experiment; however, $(L/S)_c$ and $(L/S)_i$ are related to the chain structure and interchain interaction, which cannot be measured directly. If the conductivity of oriented films (σ') also obeys eq. (6), then,

$$\sigma'_m = \frac{\sigma'_c\sigma'_i}{a'\sigma'_i + b'\sigma'_c} \tag{7}$$

where

$$\left(\frac{S'}{L'}\right)_m\cdot\left(\frac{L'}{S'}\right)_c = a' \tag{7a}$$

$$\left(\frac{S'}{L'}\right)_m\cdot\left(\frac{L'}{S'}\right)_i = b' \tag{7b}$$

where the physical meaning of σ'_c, σ'_i, a', and b' are similar to σ_c, σ_i, a, and b, respectively. So, the ratio of the measured conductivity of oriented films to unoriented films is expressed as

$$\left(\frac{\sigma'_m}{\sigma_m}\right)_{\text{theory}} = \frac{b}{b'}\cdot\left(\frac{\sigma'_i}{\sigma_i}\right)\cdot\frac{\left(\frac{a}{b}\cdot\frac{\sigma_i}{\sigma_c}+1\right)}{\left(\frac{a'}{b'}\cdot\frac{\sigma'_i}{\sigma'_c}+1\right)} \tag{8}$$

If $\sigma_c \gg \sigma_i$ and $\sigma'_c \gg \sigma'_i$ are assumed and $(a/b)(\sigma_i/\sigma_c) \to 0$ and $(a'/b')(\sigma'_i/\sigma'_c) \to 0$ are observed, then eq. (8) will be reduced to

$$\left(\frac{\sigma'_m}{\sigma_m}\right)_{\text{theory}} \doteq \frac{b}{b'}\cdot\frac{\sigma'_i}{\sigma_i} \tag{9}$$

As shown in eq. (8), one can see that the enhanced conductivity for oriented films not only depends on the chain conductivity and the interchain conductivity before and after stretching, but also on parameters $a(a')$ and $b(b')$, which are related to interchain coupling. As shown in eq. (9), however, one can see that the enhanced conductivity for stretched films is controlled mainly by the interchain conductivity (σ and σ') and the interchain coupling (b and b') when $\sigma_c \gg \sigma_i$ and $\sigma_c \gg \sigma_i$ are satisfied.

In our experiment, the enhanced conductivity along the elongation direction for oriented PANI films can be expressed by an experimental formula as

$$(\sigma_m)^{\parallel}_{\text{expt}} = \sigma_m + \alpha \cdot \frac{l}{l_0} \tag{10}$$

and

$$(\sigma_m)^{\perp}_{\text{expt}} = \sigma_m \tag{11}$$

where σ_m is the conductivity of the unstretched samples, and l_0 and l are the length of samples before and after stretching, respectively. α is a constant related to the slope of linear $(\sigma'_m)_{\text{expt}}$ plotted to l/l_0. By comparison of eq. (10) with (9), it is suggested that the enhanced PANI films may be due increasing of the interchain conductivity caused by increasing of the interchain coupling after stretching.

In addition, if the conditions of $\sigma_c \gg \sigma_i$ and $\sigma'_c \gg \sigma'_i$ are satisfied, then eqs. (6) and (7) will be reduced to eqs. (12) and (13) as

$$\sigma_m \doteq \frac{\sigma_i}{b} \tag{12}$$

and

$$\sigma'_m \doteq \frac{\sigma'_1}{b'} \tag{13}$$

Thus, it is expected that the conductivity of stretched PANI films with temperature is also controlled by a change of the interchain conductivity with conductivity. This is consistent with the experiment results in that both the unoriented and oriented PANI films show a semiconducting behavior although the conductivity of oriented films is almost two orders of magnitude higher than that of unoriented films.

CONCLUSIONS

In summary: (1) The composition of oriented PANI films is similar to that of unoriented films; on the other hand, it was demonstrated by polarized FTIR spectra, SEM, and X-ray diffraction that the chain and/or interchain were oriented along the stretching direction after the drawing treatment. (2) The conductivity of oriented PANI films parallel to the elongation direction is proportional to the elongation ratio; however, its conductivity perpendicular to the elongation direction is independent of the elongation ratio. A maximum conductivity at room temperature can be achieved up to 500 s/cm with conductivity anisotropy as high as 20 : 1. (3) The temperature dependence of conductivity at 77–300 K and at applied pressure of 0–11.4 kbar for both unoriented and oriented PANI films is consistent with the 3-D variable-range hopping model. For oriented PANI films, however, the hopping barrier, T_0, is one order magnitude lower than that of unoriented films. This is consistent with the fact that the chain and/or interchain for oriented PANI films is oriented along the elongation direction after drawing processes. (4) A simple model of a series of chain conductivity and interchain conductivity are proposed to explain the enhanced conductivity along the elongation direction for oriented films.

This work was supported by NFSC and Chinese Academy of Sciences.

REFERENCES

1. K. R. Cromack, M. E. Jozefowize, J. M. Ginder, R. P. McCall, A. J. Epstein, E. M. Scherr, and A. G. MacDiarmid, *Bull. Am. Phys. Soc.*, **34,** 583 (1989).
2. K. R. Cromack, M. E. Jozetowicz, J. M. Ginder, A. J. Epstein, R. P. McCall, G. Du, J. M. Leng, K. Kim, and C. Li, *Macromolecules,* **24,** 4157 (1991).
3. E. M. Scherr, A. G. MacDiarmid, S. K. Manohar, J. G. Masters, Y. Sun, X. Tang, M. A. Druy, P. J. Glatkowski, V. B. Cajibe, J. E. Fis, K. R. Cromack, M. E. Jozefowicz, J. M. Ginder, R. P. McCall, and A. J. Epstein, *Synth. Met.,* **41,** 735 (1991).
4. A. P. Monkman and P. Adams, *Synth. Met.,* **41–43,** 891 (1991). A. P. Monkman and P. Adams, *Synth. Met.,* **40,** 87 (1991).
5. A. G. MacDiarmid, J. C. Chang, M. Halpern, W. S. Mu, N. L. Somasiri, W. Wu, and S. I. Yaniger, *Mol. Cryst. Liq. Cryst.,* **121,** 187 (1985).
6. M. Wan, Y. Cao, J. Li, W. Zhou, and S. Li, *Chin. J. Polym. Sci.,* **9**(3), 209 (1991).
7. M. E. Jozefowicz, A. J. Epstein, J. P. Pouget, J. G. Master, A. Ray, Y. Sun, X. Tang, and A. G. MacDiarmid, *Synth. Met.,* **41,** 779 (1991).
8. Y. B. Moon, Y. Cao, P. Smith, and A. J. Heeger, *Polym. Commun.,* **30,** 196 (1989).
9. Z. H. Wang, E. M. Scherr, A. G. MacDiarmid, and A. J. Epstein, *Phys. Rev.,* **45,** 4190 (1992).
10. M. Wan, W. Zhou, and Y. Li, *Chin. J. Polym. Sci.,* **9**(4), 307 (1991).
11. M. Wan, W. Zhou, and Y. Li, *Solid State Commun.,* **81**(4), 313 (1992).

12. N. F. Mott and E. A. Davis, *Electronic Processes in Non-crystalline Materials,* Clarendon Press, Oxford, 2nd ed., 1979, p. 34.
13. Z. H. Wang, C. Li, E. M. Scherr, A. G. MacDiarmid, and A. J. Epstein, *Phys. Rev.,* **66,** 1745 (1991).
14. A. P. Monkman and P. Adams, *Synth. Met.,* **41,** 627 (1991).
15. F. Zuo, M. Angelopoulos, A. G. MacDiarmid, and A. J. Epstein, *Phys. Rev.,* **36,** 3475 (1987).
16. L. W. Shacklette and R. H. Baughman, *Mol. Cryst. Liq. Cryst.,* **189,** 193 (1991).
17. P. Sheng, B. Abeles, and Y. Arie, *Phys. Rev. Lett.,* **31,** 44 (1973).
18. P. Sheng and B. Abeles, *Phys. Rev. Lett.,* **34,** 28 (1992).
19. R. H. Baughman and L. W. Shacklette, *J. Chem. Phys.,* **90,** 7492 (1989).
20. R. H. Baughman and L. W. Shacklette, *Phys. Rev. B,* **39,** 5872 (1989).
21. J. M. Ginder, A. J. Epstein, and A. G. MacDiarmid, *Synth. Met.,* **29,** E395 (1989).
22. L. B. Coleman, *Rev. Sci. Instr.,* **49,** 58 (1978).
23. M. Wan, *Chin. J. Polym. Sci.,* **7**(4), 330 (1988).
24. M. Wan, P. Wang, Y. Cao, and R. Qian, *Solid State Commun.,* **47,** 759 (1983).
25. P. Wang, M. Wan, X. Bi, Y. Yao, and R. Qian, *Acta Phys. Sin.,* **3,** 1771 (1984).
26. Y. Cao, P. Wang, and R. Qian, *Makromol. Chem.,* **186,** 1093 (1985).

Received December 2, 1992
Accepted January 6, 1994